Eur. Phys. J. D **38**, 185–191 (2006)
DOI: 10.1140/epjd/e2005-00303-6

THE EUROPEAN PHYSICAL JOURNAL D

Steric and energetic properties of the Cl^-–C_6H_6–Ar_n heterocluster

M. Albertí[1], A. Castro[2], A. Laganà[2,a], M. Moix[2], F. Pirani[2,4], and D. Cappelletti[3,4]

[1] CERQT, Departament de Química Física, Parc Científic, Universitat de Barcelona, C/ Martí i Franquès 1, 08028 Barcelona, Spain
[2] Dipartimento di Chimica, Università di Perugia, 0123 Perugia, Italy
[3] Dipartimento di Ingegneria Civile ed Ambientale, Università di Perugia, 0123 Perugia, Italy
[4] INFM, Unità di Perugia, 0123 Perugia, Italy

Received 18 July 2005 / Received in final form 31 August 2005
Published online 16 November 2005 –

Abstract. The dynamics of heteroclusters containing argon, benzene and chlorine has been investigated using a recently proposed potential energy functional that takes into account both the electrostatic and the non-electrostatic contributions to the overall noncovalent interaction. Related steric and energetic properties are compared with those homologous cationic clusters.

PACS. 31.15.Qg Molecular dynamics and other numerical methods – 34.20.Gj Intermolecular and atom-molecule potentials and forces – 34.30.+h Intramolecular energy transfer; intramolecular dynamics; dynamics of van der Waals molecules

1 Introduction

In recent times, there has been increasing interest in investigating clusters and related interactions of relevance for chemical and biochemical processes, with a particular attention for molecular recognition and selection [1–31]. In this perspective we have recently extended to ion benzene (bz) rare-gas systems an atom-bond type formulation of the interaction originally developed for pure bz rare-gas systems [32,33]. The strength of this formulation of the interaction lies in the closed relationship existing between its parameters and some basic physical properties of the few body fragments of the overall molecular aggregate and in the fact that two-body atom-bond formulations of the interaction incorporate in a natural way three-body effects. Indeed, a composition of atom(ion)-bond functionals has been already found to properly describe the potential energy surface (PES) and related steric and energetic features of alkali ion benzene systems alone or solvated by rare gas atoms. This has allowed, so far, to calculate both static and dynamic properties of the K^+–bz–Ar_n clusters [34] and to evidence their specific steric biases with respect to those of bz–Ar_n [18,19].

In this paper we discuss the extension of the atom-bond treatment to clusters containing the Cl^- anion and compare their static and dynamic properties with those of their K^+–bz–Ar_n homologues with n varying from 1 to 3. The chemistry of anions containing clusters is much less studied than that of cations containing ones. This stems out of the intuitive mind that the charge distribution, associated with the π electronic cloud of the aromatic ring, stabilizes the cation-bz clusters (because of the attractive nature of the related electrostatic interaction) while destabilizing the anion-bz ones (because of the repulsive nature of the related electrostatic interaction). Yet, the recent design of new receptors stereoselectively binding anionic guests has fuelled a revisitation of this topic [35–37]. This has fostered, for example, increasing attention to the problem of ion-pair recognition in the field of coordination chemistry [37] and of stereoselective simultaneous complexation of cationic and anionic guest species by multisite receptors. In both cases, in fact, one needs an accurate description of the interaction of negatively charged guests with various receptors.

The paper is articulated as follows: in Section 2 a description of the atom-bond PES of the Cl^-–bz–Ar_n heterocluster and the analysis of its static properties are given, in Section 3 the main dynamical properties of the Cl^-–bz–Ar_n clusters (for a rigid benzene) are analyzed and compared with those of K^+–bz–Ar_n. Concluding remarks are given in Section 4.

2 The potential energy surface

As already mentioned the main goal of our work was to investigate the possibility of extending the atom(ion)-bond formulation of the interaction to the description of the Cl^-–bz–Ar_n systems and rationalizing the steric and energetic features of the related PES.

[a] e-mail: lag@dyn.unipg.it

2.1 The functional representation of the interaction

In the present study the benzene molecule is assumed to be rigid (because of the low temperature range considered) and the overall interaction (V_{total}) is built up of the electrostatic (V_{el}) and the non electrostatic (V_{nel}) contributions (each expressed using a suitable functional form).

V_{el} arises from the interaction between the charge of the ion and the charges assigned to the molecular frame to asymptotically reproduce the molecular quadrupole. Accordingly, V_{el} is assembled by placing negative charges above and below (with respect to the molecular plane) the C atoms of benzene and by placing positive charges on the H atoms [34]. All these charges interact with the ion via Coulombic potentials. This is a key feature of the interaction and plays an important role in differentiating the energetic and steric properties of the Cl^-–bz–Ar_n heteroclusters from those of K^+–bz–Ar_n.

V_{nel} is the component of the interaction more difficult to formulate, because it results from the balancing of both dispersion and induction attraction, dominant at long range, with exchange (size) repulsion, dominant at short range. Our choice is based on the following considerations:

(i) polarizability is the key property to scale attraction or repulsion in molecular systems [38] by taking it as a sum of bond components [40];
(ii) the dispersion/induction center can be identified, for bonds like C–C and C–H, as the center of the bond [32];
(iii) an atom (ion)-bond functional form suitably represents pairwise interactions since it removes most of the drawbacks of the usual atom-atom formulations and can be easily correlated to polarizability [32,34].

In the atom(ion)-bond representation, V_{nel} is given by the following atom(ion)-bond interaction terms: $6n$ Ar–CCbond, $6n$ Ar–CHbond, 6 Cl^-–CCbond and 6 Cl^-–CHbond. It also contains the following atom(ion)-atom terms $n(n-1)/2$ Ar–Ar and n Cl^-–Ar. Each term takes the following functional form

$$V(r,\alpha) = \varepsilon(\alpha)\left[\frac{m}{n(r,\alpha)-m}\left(\frac{r_0(\alpha)}{r}\right)^{n(r,\alpha)} - \frac{n(r,\alpha)}{n(r,\alpha)-m}\left(\frac{r_0(\alpha)}{r}\right)^{m}\right] \quad (1)$$

where r is the distance of either the atom or the ion from the center of the bond and α is the angle formed by the **r** vector with the bond. For each atom(ion)-bond pair the parameters ε (the potential well depth) and r_0 (the location of the minimum of the well) are expressed as a combination of a parallel, $\varepsilon_{\|}$ and $r_{0\|}$, and a perpendicular, $\varepsilon_{\perp}$ and $r_{0\perp}$, contribution [32,34]. Related equations are

$$\varepsilon(\alpha) = \varepsilon_{\perp}\sin^2(\alpha) + \varepsilon_{||}\cos^2(\alpha), \quad (2)$$

$$r_0(\alpha) = r_{0\perp}\sin^2(\alpha) + r_{0||}\cos^2(\alpha). \quad (3)$$

Table 1. Atom(anion)–atom interaction parameters.

atom$\cdots$atom	ε/meV[a]	r_0/Å[a]	m
Ar$\cdots$Ar	12.34	3.76	6
Ar$\cdots$$Cl^-$	76.00	3.77	4

[a] Same values as in references [38,39].

Table 2. Atom(anion)–bond interaction parameters.

atom$\cdots$bond	$\varepsilon_{\perp}$/meV	$\varepsilon_{||}$/meV	$r_{0\perp}$/Å	$r_{0||}$/Å	m
Ar$\cdots$C–C[a]	3.895	4.910	3.879	4.189	6
Ar$\cdots$C–H[a]	4.814	3.981	3.641	3.851	6
$Cl^-\cdots$C–C	16.37	59.64	3.832	4.073	4
$Cl^-\cdots$C–H	25.48	28.60	3.655	3.839	4

[a] Same values as in reference [32].

The m parameter, determining the dependence on r of the long range attraction, is taken, as usual, to be 6 or 4 depending on the leading term of the multipole expansion of the dispersion and induction interaction, respectively.

The parameter n, determining the strength both of the long range attraction and of the short range repulsion, is expressed as a function of both r_0 and r using the equation

$$n(r,\alpha) = \beta + 4.0\left(\frac{r}{r_0(\alpha)}\right)^2 \quad (4)$$

with β being taken equal to 10.0 and 9.0 for the Ar-bond and the Cl^-–bond interactions, respectively [32].

The angular dependence of these parameters is obviously ignored for the Cl^-–Ar and the Ar–Ar pairs. Their values (the usual atom-ion and atom-atom ones), obtained as described in references [38,39], are given in Table 1. The remaining atom-bond and ion-bond parameters, obtained following the procedure described in reference [40] and extended in reference [34], are given in Table 2.

2.2 The static properties of the potential energy surface of the Cl^-–bz cluster

In this section, the steric and energetic properties of the Cl^-–bz cluster are discussed by comparing calculated with measured properties and by analyzing the isoenergetic contours of V_{total} ($V_{total} = V_{el} + V_{nel}$) given in Figure 1. As to the comparison with the experiment it is found that the most stable geometry given by the PES is in good agreement with the one obtained by an analysis of recent spectroscopic observations [41]. Moreover, the binding energy and the equilibrium distance reasonably well agree with ab initio predictions [41,42] and with results obtained from thermodynamical investigations [42].

The isoenergetic contours of the PES, shown in the left hand side panels of Figure 1 (upper panel for approaches perpendicular to the aromatic ring, lower panel for the on plane ones), show that there are significant differences between steric properties of Cl^-–bz and those of K^+–bz (related contours are shown in the corresponding right hand side panels). As an example, for K^+–bz

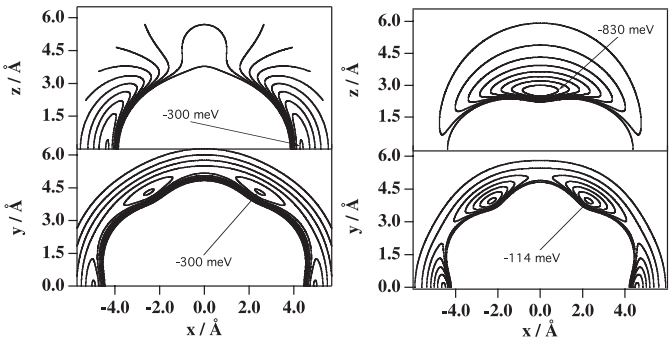

Fig. 1. Isoenergetic contours of the potential energy surface of the Cl^-–bz (left hand side panels) and K^+–bz (right hand side panels) systems. The benzene molecule lies on the xy-plane. The corresponding ion approaches the benzene center of mass either perpendicularly to the aromatic ring (see the upper panels) along the z-axis (i.e., along the C_6 axis of symmetry) or on-plane (see the lower panels). Energy contours are spaced by 40 meV in the upper left panel and by 30 meV in the lower left panel for Cl^-–bz and by 100 meV (upper right panel) and 15 meV (lower right panel) for K^+–bz.

Table 3. Electrostatic and non-electrostatic energies and distance R from ion to the center of the benzene, for the Cl^-–bz and K^+–bz clusters in their most stable configuration.

Cluster	R/Å	V_{el}/meV	V_{nel}/meV
Cl^-–bz	4.94	−108	−197
K^+–bz	2.69	−636	−291

the most stable configuration was found when the cation approaches benzene perpendicularly to the aromatic ring while this is not true for Cl^-–bz. In fact, the potential energy surface of the Cl^-–bz cluster is highly repulsive when Cl^-approaches along the C_6 symmetry axis of benzene. Accordingly, the most stable Cl^-–bz configuration has a six fold degenerate on-plane geometry. On-plane stable geometries do, indeed, exist also for cationic clusters. However, because of the different role of V_{el} and V_{nel} and of the higher stabilization energy, out of plane geometries are largely preferred by the K^+ cation that usually sits on the C_6 symmetry axis of benzene. The energy associated with the Cl^-–bz minimum, is compared in Table 3 with that of K^+–bz. As apparent from the table, the energy of the Cl^-–bz minimum is about 620 meV higher than that of the most stable (out of plane) geometry of the K^+–bz cluster. As it is possible to infer from Table 3, the value of V_{total} at the equilibrium configuration is mainly determined by the non-electrostatic component (V_{nel} accounts for about 60% of the total intermolecular energy). This is in contrast with what is found for the K^+–bz cluster for which V_{el} accounts for about 70% of V_{total} [34].

2.3 The static properties of the potential energy surface of the Cl^-–bz–Ar_n clusters

The analysis of the atom-bond PES has been extended to that of the rare-gas atom solvated ion-benzene clusters.

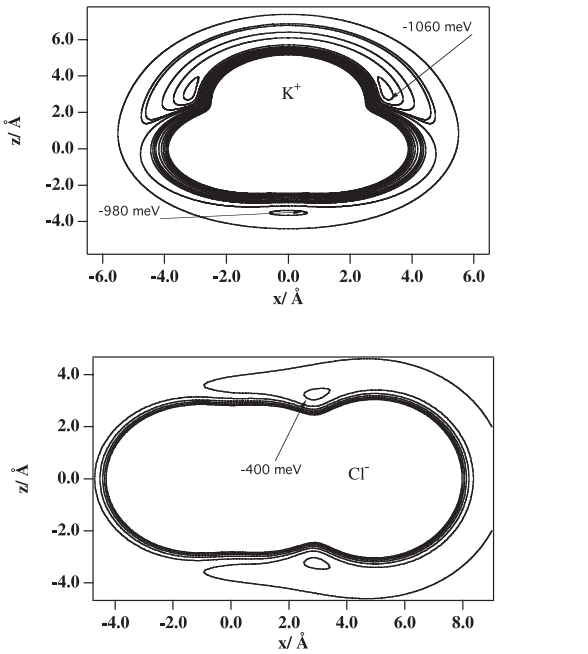

Fig. 2. Isoenergetic contours of the potential energy surface for the Cl^-–bz–Ar (lower panel) and K^+–bz–Ar (upper panel) clusters. The benzene molecule lies on the xy-plane. The Cl^-–bz and K^+–bz systems are kept fixed at their equilibrium geometries. The Ar atom is allowed to move around on the xz-plane. Energy contours for Cl^-–bz–Ar and K^+–bz–Ar are spaced respectively by 50 meV and 25 meV. The curve taken at –980 meV has been individually labeled to emphasize the structure of the possible isomers.

In this case too, the properties of the PES of the anionic cluster are compared with those of the cationic cluster. Accordingly, the potential energy contours of Cl^-–bz–Ar and of K^+–bz–Ar are given respectively in the lower and in the upper panels of Figure 2. As shown by the upper panel of the figure, for K^+–bz–Ar there are two stable geometries associated with two different minima leading to the formation of two isomers (for the most stable of them, K^+ and Ar are located on the same side of the plane of the benzene ring, while for the less stable, K^+ and Ar are located on opposite sides). On the contrary, the lower panel shows that the Cl^-–bz–Ar cluster has only one stable geometry, with Cl^- placed on the plane of the aromatic ring and the Ar atom floating out of plane. The shape of the Cl^-–bz–Ar cluster at the equilibrium geometry is sketched in Figure 3. The figure shows that the Ar atom is placed half way between the benzene ring and the chlorine ion so as to be stabilized by both interactions. Similar differences are also observed when cationic and anionic clusters contain more than one Ar atom. The K^+–bz clusters solvated by more than one Ar atoms show stable structures with the Ar atoms and K^+ placed on the same or on different sides of the aromatic ring. On the contrary, anionic clusters solvated by the Ar atoms only show stable configurations when Cl^- is placed on the plane of the benzene molecule. When including Ar atoms various isomers can be formed with Ar placed on different sides of the

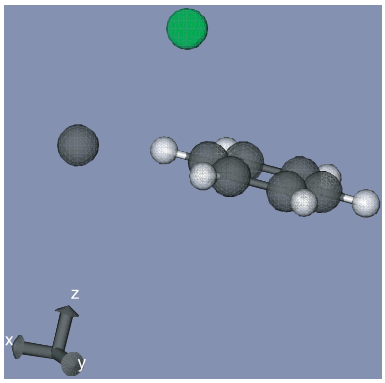

Fig. 3. Equilibrium configuration for the Cl^-–bz–Ar cluster. The benzene is placed on the xy-plane and the Cl^- and Ar are placed respectively at (4.94, 0, 0) and (2.9, 0, 3.2). Distances are given in Å.

Table 4. Equilibrium configuration energy, V_{cfg}, and energy contributions from electrostatics, V_{el}, non electrostatic including ion-benzene, $V_{\mathrm{Cl^-\!-bz}}$, benzene–Ar, $V_{\mathrm{bz-Ar}(n)}$ and the sum of atom-atom and atom-ion pair interactions, V_{pair}, for the Cl^-–bz–Ar_n clusters (n = 1, 2, 3). All energy contributions are expressed in meV.

Isomer	V_{cfg}	V_{el}	$V_{\mathrm{Cl^-\!-bz}}$	$V_{\mathrm{bz-Ar}(n)}$	V_{pair}
Cl^-–bz–Ar	−411	−108	−197	−30	−76
Cl^-–bz–Ar_2	−516	−108	−197	−59	−152
Cl^-–bz–Ar_3	−625	−108	−197	−68	−252

aromatic ring (though never in the position exactly opposite to that of Cl^-). The various contributions to the total energy of the solvated clusters, obtained from dynamical simulations (see next section), are given in Table 4.

3 The molecular dynamics investigation

As in our previous studies on bz–Ar_n [19,33] and K^+–bz–Ar_n [34] clusters, the dynamics of Cl^-–bz–Ar_n on the atom (ion)-bond PES has been investigated using the DL_POLY suite of programs [43]. Dynamical simulations have been performed by considering a microcanonical ensemble (NVE) of atoms and treating the benzene molecule as a rigid body. The calculations at different energy values have been carried out by looping over increasing values of the total energy, E_{total}, defined as the sum of the kinetic (E_k) and the potential energy of the cluster. At each new energy we start the simulation from the configuration, the velocities and the forces obtained from the last step of the previous run. A time step of 1 fs has been used to integrate the dynamics equations, so as to keep the fluctuations of total energy smaller than 10^{-5} eV. The temperature, T, has been calculated from the relationship $T = 2E_k/k_B f$ (with k_B being the Boltzmann constant and f being the number of degrees of freedom of the system) by neglecting the zero point energy. The total integration time for the simulations was set at 25 ns. This time is long enough to ensure that the mean value of temperature and of the various energy contributions do not vary when extending the calculations to longer times. No cutoff radius has been set when calculating the interaction.

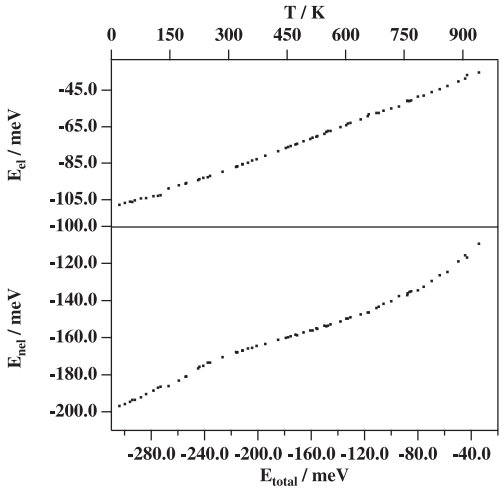

Fig. 4. The variation of E_{el} (upper panel) and E_{nel} (lower panel) components plotted as a function of E_{total} and T.

As discussed in reference [34], to help the rationalization of the results (see the following subsections) the configuration energy (E_{cfg}) of the cluster (defined as an average of the potential energy of the cluster over all the accessible configurations at the chosen total energy) was calculated and analyzed. To this end also the analysis of both the electrostatic (E_{el}) and the non electrostatic (E_{nel}) components of E_{cfg} (as well as the sum of the energy of the asymptotic fragments) were analyzed. The values of the various contributions (extrapolated to $T = 0$ K where they coincide with the specific V components) are given in Table 4 where, for completeness, also V_{pair}, defining the sum of the atom (ion)-atom interactions, is given.

3.1 The dynamics of the Cl^-–bz cluster

Several dynamical simulations have been performed by increasing the total energy (and consequently T) of the system. Simulations have been performed for temperatures ranging from $T = 2$ K to $T = 950$ K. The Cl^-–bz cluster was found to be very stable up to $T = 850$ K. At higher temperatures the cluster becomes unstable and the dissociation probability increases substantially (on the contrary, for the K^+–bz cluster the probability of dissociating stays low up to temperatures of about 2500 K). This is not surprising due to the already discussed differences in the corresponding interaction potentials and stabilization energies of the two clusters (the cationic cluster is much more stable than the anionic one). The plot of the various components of E_{cfg} is, in this regard, of particular help. For this reason the variation of E_{el} (upper panel) and E_{nel} (lower panel) contributions to E_{cfg} are plotted in Figure 4 as a function of E_{total}. As can be easily seen from the figure, in spite of the different value of the two components, their dependence on total energy is similar. This

sharply contrasts with the behavior of the same quantities for the K^+–bz cluster [34]. In fact, for K^+–bz at high temperatures, before dissociation, the E_{nel} remains nearly unchanged as E_{total} increases. These differences can be interpreted in terms of the different dynamics of the ion in the two clusters. In particular, in the case of Cl^-–bz, the stretching is boosted by the fact that the potential energy pushes away the Cl^- ion. Accordingly, although no appreciable changes in the orientation are produced, an increase of the average distance of Cl^- from the center of mass of the benzene is observed. This motion leads to a comparable variation of the two contributions (electrostatic and non electrostatic) to the configuration energy. On the other hand, in the K^+–bz system, both components of the potential energy are very strong (see Tab. 3) and a variation of the stretching motion is quite unlikely to occur. As a result, the cluster deforms in a way that allows the exploration of regions of the PES in which different variations of the two energy contributions can occur.

3.2 The dynamics of the Cl^-–bz–Ar_n clusters

Significant differences have also been found between the dynamics of Ar solvated cation- and anion–bz clusters. As already seen from the discussion on the Cl^-–bz clusters, the analysis of the dynamical features can be carried out by inspecting the magnitude of the different components of the interaction. In fact, while the bz–Ar, Cl^-–Ar and K^+–Ar interactions have approximately the same order of magnitude, that of the ion–bz is definitely larger. Accordingly, the ion typically tends to stay very close to the equilibrium position. On the contrary the Ar atom, being tied to the system through a weaker interaction, moves around more freely. Consequently, in the Cl^-–bz–Ar_n and K^+–bz–Ar_n clusters, the Ar atoms tend to move around Cl^- and around K^+, respectively. In the case of K^+–bz–Ar clusters the Ar atom moves preferentially around the C_6 axis. In particular, at low total energy, the Ar atom circles around the C_6 axis, at a distance about the r_0 value (3.19 Å) of the K^+–Ar potential. This motion does not affect the variation of E_{cfg}. When the total energy increases, the Ar atom can be displaced to the opposite side of the aromatic ring and the system isomerizes. On the contrary, in the case of the Cl^-–bz–Ar clusters, a motion of Ar around Cl^- would lead to a large increase of the configuration energy. Thus in this cluster, at low energy, the Ar atom is confined to oscillate near the equilibrium configuration. At higher total energy the Ar atom can reach other regions of the PES in which it is stabilized only by the interaction with chlorine. In this case, the contribution of Ar to the interaction energy decreases, and the probability of dissociating increases. As a matter of fact, the dynamical studies show that the Ar atoms tend to move close to Cl^- while it vibrates (nearly on plane with the aromatic ring).

The variation of the different energy terms as a function of total energy is shown in Figure 5 for Cl^-–bz–Ar (a similar behaviour is obtained for clusters containing more than one Ar atom). The main difference between

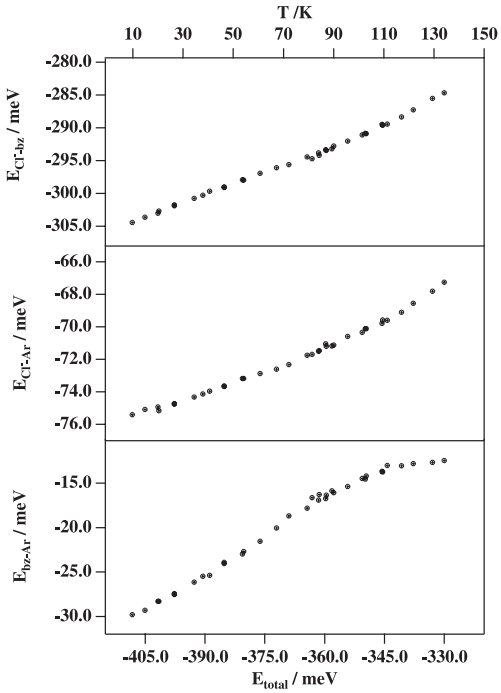

Fig. 5. The contributions $E_{\mathrm{Cl^-\!-bz}}$, $E_{\mathrm{Cl^-\!-Ar}}$ and $E_{\mathrm{bz-Ar}}$ of the Cl^-–bz–Ar cluster plotted as a function of E_{total} and T.

Table 5. Mean temperature (T), number of changes of some Ar atoms from one side to the other of the benzene plane (changes Ar) and ratio of the time spend for the clusters with Ar atoms placed in different side (tds) and in the same side (tss) on the benzene plane of the Cl^-–bz–Ar_3 cluster.

T/K	changes Ar	tds/tss
40.8	2	0.21
47.3	22	0.51
50.1	28	0.54
51.3	35	0.67
53.6	49	0.70
56.9	87	0.96

the Cl^-–bz–Ar_n and the K^+–bz–Ar_n clusters [34], lies in the fact that for anionic clusters (contrary to what is observed for cationic ones), there is not appreciable change in the dependence of the interaction energy between Ar and Cl^- when E_{total} increases. This is due to the fact that no isomerization occurs for Cl^-–bz–Ar_n as evidenced by the absence of a change in slope of the plot of $E_{\mathrm{Cl^-\!-Ar}}$ versus total energy. For example, in the case of Cl^-–bz–Ar_3 the ratio of the time spent by the system in configurations having all the Ar atoms on the same side (tss) and in those having the Ar atoms on different sides (tds) of the benzene plane has been calculated together with the number of times that the Ar atoms switch from one side of the aromatic plane to the other. The results (see Tab. 5) show that even at very low temperature the ratio between the tds and tss times tends to one as T increases. This indicates, like in the case $n = 3$ shown the table, that the Ar atoms increasingly tend to move in a random fashion

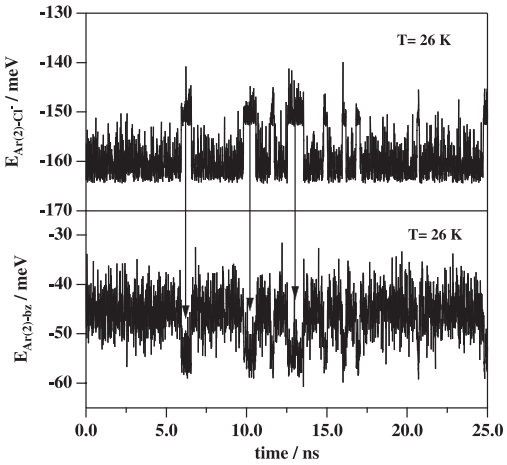

Fig. 6. Time evolution of the $E_{\mathrm{Ar}(2)-\mathrm{Cl}}-$ (upper panel) and $E_{\mathrm{Ar}(2)-\mathrm{bz}}$ (lower panel) interaction energies for the Cl^-–bz–Ar_2 cluster during a 25-ns simulation at $E_{total} = -496$ meV.

about Cl^-. This finds a rationale in the energetic of the involved processes and in the topology of the potential energy surface. In fact, the internal degrees of freedom evolve in a way that at a given total energy, lower is the potential energy associated with the Cl^-–Ar_n fragment, larger is that of the bz–Ar_n one. This means that when an Ar atom gets near the ion (and consequently to the benzene plane) the approaching path is such that the interaction between Cl^- and Ar roughly increases as much as that between benzene and Ar decreases. Accordingly, the overall potential energy of the configuration tends to remain, on the average, constant. This is confirmed by the values of the Cl^-–Ar_n and bz–Ar_n ($n = 2$) interaction energies plotted in Figure 6 as a function of the simulation time at $T = 26$ K. The maxima observed for a certain contribution systematically correspond to the minima for the other. Such behavior has been also observed at higher temperatures and for clusters containing more Ar atoms. This confirms what is usually expected from a solvation process: the solvent molecules (from few to many) rearrange themselves in a way to compensate for the variation of the molecular geometries of the solute.

4 Conclusions

In this paper, the interaction of the Cl^-–C_6H_6–Ar_n aggregates has been formulated for the first time in terms of atom(ion)-bond functionals. This leads to an accurate reproduction of the asymptotic fragmentation limits and allows a rationalization of the steric and energetic properties of anionic heteroclusters. The related studies of the static and dynamic properties of the system have confirmed the suitability of the atom(ion)-bond functional to describe steric and energetic properties of heteroclusters (thanks to its intrinsic three body nature), with relatively small computational effort. The paper also points out that the atom-bond functional is able to single out the key differences between cationic and anionic interactions.

A first important element of difference between Cl^-– and K^+–bz clusters is the fact that for Cl^-–bz the E_{el} and E_{nel} contributions to E_{cfg} are almost equal and remain so while E_{total} increases. On the contrary, in the case of K^+–bz E_{el} is responsible for most of the variation of E_{total}. Our study also describes some important differences in the dynamics of Cl^-– and K^+–bz clusters. A second important element of difference between Cl^-–bz–Ar_n and K^+–bz–Ar_n clusters is the fact that for the former Cl^- tends to sit on the plane of the aromatic ring (because the potential energy surface is very repulsive for out of plane geometries) whereas for the latter K^+ is firmly placed above the aromatic ring (on the C_6 rotational axis) implying the possibility of displacing the Ar atom on the other side of the benzene ring. The paper has further discussed the differences in the steric properties of the anionic and cationic clusters in terms of the various energy contributions to the interaction and of the shape of the potential energy surface. For K^+ clusters the possibility of isomerizing and therefore of opening new portions of the phase space was found to lead at certain temperatures to a change of slope in the plots of the various contributions to E_{cfg} as E_{total} increases. On the contrary, for the Cl^- clusters in which the phase space does not change significantly, the energetic variations occur in a way that reciprocally compensates leading to an adiabatic-like evolution. This seems to indicate that systems containing anions may tend to tie benzene rings in a sheet, while those containing cations tend to tie them on a pile.

M. Albertí acknowledges financial support from the Spanish DGICYT (Project CTQ2004-01102) and from the Generalitat de Catalunya-DURSI project (2001SGR-00041). Also thanks are due to the Centre de Supercomputació de Catalunya CESCA-C^4 for use of their computational facilities. EU support through the MCInet Research Training Network ("Generation, Stability and Reaction Dynamics of Multiply Charged Ions in the Gas Phase", contract No. HPRN-CT-2000-00027) and COST in Chemistry Action D23 is also acknowledged. The research has also been supported by MIUR, CNR and ASI.

References

1. K. Müller-Dethelfs, P. Hobza, Chem Rev. **100**, 143 (2000)
2. J.L. Alonso, S. Antolínez, S. Bianco, A. Lesarri, J.C. López, W. Caminati, J. Am. Chem. Soc. **126**, 3244 (2004)
3. V. Aquilanti, E. Cornicchi, M. Moix Teixidor, N. Saendig, F. Pirani, D. Cappelletti, Angew. Chem. Int. Ed. **44**, 2336 (2005)
4. C.E. Dykstra, J.M. Lisy, J. Mol. Struc. (Theochem) **500**, 375 (2000)
5. M.J. Ondrechen, Z. Berkovitch-Yellin, J. Jortner, J. Am. Chem. Soc. **103**, 6586 (1981)
6. L.E. Fried, S. Mukamel, J. Chem. Phys. **96**, 116 (1991)
7. M. Schmidt, J. Le Calvè, M. Mons, J. Chem. Phys. **98**, 6102 (1993), and references therein
8. M. Mons, A. Courty, M. Schmidt, J. Le Calvè, F. Piuzzi, I. Dimicoli, J. Chem. Phys. **106**, 1676 (1997)
9. D.C. Easter, L. Bailey, J. Mellot, M. Tirres, T. Weiss, J. Chem. Phys. **108**, 6135 (1998)

10. M. Schmidt, M. Mons, J. Le Calvè, Chem. Phys. Lett. **177**, 371 (1991)
11. Th. Brupbacher, J. Makarewicz, A. Bauder, J. Chem. Phys. **101**, 9736 (1994)
12. P. Hobza, O. Bludsky, H.L. Selzle, E.W. Schlag, Chem. Phys. Lett. **250**, 402 (1996)
13. T. Lenzer, K. Luther, J. Chem. Phys. **105**, 10944 (1996)
14. V. Bernshtein, I. Oref, J. Chem. Phys. **112**, 686 (2000)
15. J. Vacek, K. Konvicka, P. Hobza, Chem. Phys. Lett. **220**, 85 (1994)
16. J. Vacek, P. Hobza, J. Phys. Chem. **98**, 11034 (1994)
17. A. Dullweber, M.P. Hodges, D.J. Wales, J. Chem .Phys. **106**, 1530 (1997)
18. A. Riganelli, M. Memelli, A. Laganà, Lect. Notes Comp. Sci. **2331**, 926 (2002)
19. A. Zoppi, M. Becucci, G. Pietraperzia, E. Castellucci, A. Riganelli, M. Albertí, M. Memelli, A. Laganà, in *Clustering properties of rare gas atoms on aromatic molecules*, 16th International Symposium on Plasma Chemistry, Taormina, Italy, June 22–27, 2003
20. H. Koch, B. Fernández, J. Makariewicz, J. Chem. Phys. **111**, 198 (1999)
21. D.A. Dougherty, Science **271**, 163 (1996)
22. J.C. Ma, D.A. Dougherty, Chem. Rev. **97**, 1303 (1997)
23. S. Mecozzi, A.P. West Jr, D.A. Dougherty, in *Proceedings of the National Academy of Sciences*, USA, 1966, Vol. 93, p. 10566
24. S. Tsuzuki, M. Yoshida, T. Uchimaru, M. Mikami, J. Phys. Chem. A **105**, 769 (2001)
25. C. Felder, H.-L. Jiang, W.-L. Zhu, K.-X. Chen, I. Silman, S.A. Botti, J.L. Sussman, J. Phys. Chem. A. **105**, 1326 (2001)
26. S. Mecozzi, A.P. West, D.A. Dougherty, J. Am. Chem. Soc. **118**, 2307 (1996)
27. E. Cubero, F.J. Luque, M. Orozco, in *Proceedings of the National Academy of Sciences*, USA, 1998, Vol 95, p. 5976
28. J.W. Caldwell, P.A. Kollman, J. Am. Chem. Soc. **117**, 4177 (1995)
29. O.M. Cabarcos, C.J. Weinheimer, J.M. Lisy, J. Chem. Phys. **108**, 5151 (1998)
30. O.M. Cabarcos, C.J. Weinheimer, J.M. Lisy, J. Chem. Phys. **110**, 8429 (1999)
31. J.B. Nicholas, B.P. Hay, D.A. Dixon, J. Phys. Chem. A **103**, 1394 (1999)
32. F. Pirani, M. Albertí, A. Castro, M. Moix, D. Cappelletti, Chem. Phys. Lett. **394**, 37 (2004)
33. M. Albertí, A. Castro, A. Laganà, F. Pirani, M. Porrini, D. Cappelletti, Chem. Phys. Lett. **392**, 514 (2004)
34. M. Albertí, A. Castro, A. Laganà, M. Moix, F. Pirani, D. Cappelletti, J. Phys. Chem. A **109**, 2906 (2005)
35. C. Garau, A. Frontera, D. Quiñonero, P. Ballester, A. Costa, P.M. Deyà, Chem. Phys. Chem. **4**, 1344 (2003)
36. C. Garau, D. Quiñonero, A. Frontera, A. Costa, P. Ballester, P.M. Deyà, Chem. Phys. Lett. **370**, 7 (2003)
37. P.D. Beer, P.A. Gale, Angew. Chem. Int. Ed. **40**, 486 (2001)
38. R. Cambi, D. Cappelletti, G. Liuti, F. Pirani, J. Chem. Phys. **95**, 1852 (1991)
39. D. Cappelletti, G. Liuti, F. Pirani, Chem. Phys. Lett. **183**, 297 (1991)
40. F. Pirani, D. Cappelletti, G. Liuti, Chem. Phys. Lett. **350**, 286 (2001)
41. Z.M. Loh, R.L. Wilson, D.A. Wild, E.J. Bieske, A. Zehnacker, J. Chem. Phys. **119**, 9559 (2003)
42. K. Hiraoka, S. Mizuse, S. Yamabe, Chem. Phys. Lett. **147**, 174 (1988)
43. `http://www.dl.ac.uk/TCSC/Software/DL_POLY`